Quantum-classical correspondence in integrable systems

Yiqiang Zhao and Biao Wu

Citation: SCIENCE CHINA Physics, Mechanics & Astronomy **62**, 997011 (2019); doi: 10.1007/s11433-018-9348-2

View online: http://engine.scichina.com/doi/10.1007/s11433-018-9348-2

View Table of Contents: http://engine.scichina.com/publisher/scp/journal/SCPMA/62/9

Published by the Science China Press

SCIENCE CHINA
Physics, Mechanics & Astronomy

SCIENCE CHINA
Physics, Mechanics & Astronomy

• Article •

September 2019 Vol. 62 No. 9: 997011
https://doi.org/10.1007/s11433-018-9348-2

Quantum-classical correspondence in integrable systems

Yiqiang Zhao[1], and Biao Wu[1,2,3*]

[1] *International Center for Quantum Materials, School of Physics, Peking University, Beijing 100871, China;*
[2] *Collaborative Innovation Center of Quantum Matter, Beijing 100871, China;*
[3] *Wilczek Quantum Center, School of Physics and Astronomy, Shanghai Jiao Tong University, Shanghai 200240, China*

Received October 31, 2018; accepted December 24, 2018; published online April 23, 2019

We find that the quantum-classical correspondence in integrable systems is characterized by two time scales. One is the Ehrenfest time below which the system is classical; the other is the quantum revival time beyond which the system is fully quantum. In between, the quantum system can be well approximated by classical ensemble distribution in phase space. These results can be summarized in a diagram which we call Ehrenfest diagram. We derive an analytical expression for Ehrenfest time, which is proportional to $\hbar^{-1/2}$. According to our formula, the Ehrenfest time for the solar-earth system is about 10^{26} times of the age of the solar system. We also find an analytical expression for the quantum revival time, which is proportional to $\hbar^{-1}$. Both time scales involve $\omega(I)$, the classical frequency as a function of classical action. Our results are numerically illustrated with two simple integrable models. In addition, we show that similar results exist for Bose gases, where $1/N$ serves as an effective Planck constant.

quantum-classical correspondence, Ehrenfest time, quantum revival time, integrable systems

PACS number(s): 03.65.-w, 03.65.Sq, 02.30.Ik

Citation: Y. Zhao, and B. Wu, Quantum-classical correspondence in integrable systems, Sci. China-Phys. Mech. Astron. **62**, 997011 (2019), https://doi.org/10.1007/s11433-018-9348-2

1 Introduction

A quantum system is expected to become classical in the limit $\hbar \to 0$. However, how this exactly happens is highly nontrivial and has been studied intensively in the field of quantum chaos [1]. The issue of quantum-classical correspondence was noticed as early as in 1927 by Ehrenfest. For a particle with mass m moving in a potential $V(x)$, Ehrenfest demonstrated that the expectation values of the particle's position and momentum follow Newton-like equations [2]

$$\frac{\mathrm{d}}{\mathrm{d}t}\langle\hat{x}\rangle = \frac{\langle\hat{p}\rangle}{m}, \tag{1}$$

$$\frac{\mathrm{d}}{\mathrm{d}t}\langle\hat{p}\rangle = -\left\langle\frac{\mathrm{d}V(\hat{x})}{\mathrm{d}\hat{x}}\right\rangle, \tag{2}$$

where $\langle\cdot\rangle$ is the expectation value of the operator. These two equations are now known as Ehrenfest theorem, which offers a hint on how quantum and classical dynamics may be related. In particular, when the wave function is narrow enough and the potential $V(x)$ varies gradually in space, we approximately have $\langle\frac{\mathrm{d}V(\hat{x})}{\mathrm{d}\hat{x}}\rangle \approx \frac{\mathrm{d}V(\langle\hat{x}\rangle)}{\mathrm{d}\langle\hat{x}\rangle}$. This means that the evolution of expectation values of position and momentum would follow exactly the Newton's equation of motion. However, an initially well-localized wave packet will spread, and the expectation values of its position and momentum will eventually deviate from the classical dynamics when the width of the wave packet is no longer small. Ehrenfest time $\tau_\hbar$ is the time scale when such a quantum-classical correspondence

*Corresponding author (email: wubiao@pku.edu.cn)

breaks down [3-12]. Quantum-classical correspondence was also studied in other aspects, such as the correspondence between closed classical orbits and quantum spectra [13-16].

In this work we study systematically the quantum-classical correspondence in integrable systems. We find that the quantum-classical correspondence is characterized by two time scales, Ehrenfest time $\tau_\hbar$ and quantum revival time T_r [17-19], as shown in Figure 1. According to this figure, for a fixed Planck constant, the wave packet dynamics is almost classical when the evolution time is shorter than the Ehrenfest time $\tau_\hbar$; when the evolution time is longer than T_r, quantum revival occurs and the wave packet dynamics can no longer be approximated by semiclassical approaches. Between Ehrenfest time $\tau_\hbar$ and quantum revival time T_r, the quantum dynamics can be well approximated by classical ensemble distribution in phase space. Furthermore, we are able to derive analytical expressions for both Ehrenfest time $\tau_\hbar$ and quantum revival time T_r, both of which are intimately related to $\omega(I)$, the classical frequency as a function of classical action. We find that $\tau_\hbar \propto \hbar^{-1/2}$ and $T_r \propto \hbar^{-1}$.

For many specific systems, we find that the Ehrenfest time has a simple form $\tau_\hbar = cT_c(I/\hbar)^{1/2}$, where T_c is the period of a classical motion, I is the corresponding action, and c is a dimensionless constant of order one. Our results are applied to many concrete systems. Generally, for systems which we usually regard as quantum systems, their Ehrenfest times are short; for systems which we usually consider as classical systems, their Ehrenfest times are long. For example, for a hydrogen atom in the ground state, we have $\tau_\hbar = 0.5T_c$; for the earth orbiting around the sun, we have $\tau_\hbar = 2.3 \times 10^{36}T_c$ while the age of the solar system is only $0.5 \times 10^9 T_c$. Therefore, Ehrenfest time may be used as an indicator whether we should treat a given system as quantum or classical.

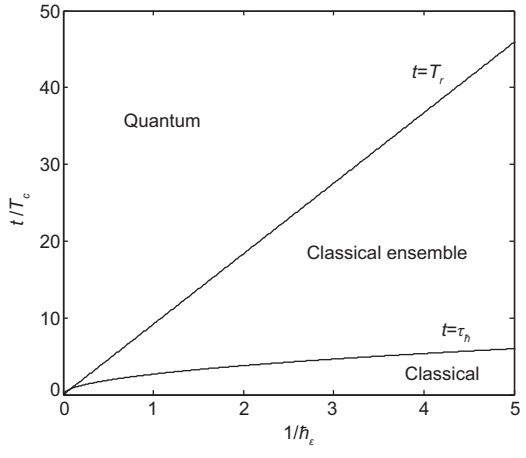

Figure 1 Ehrenfest diagram for the quantum-classical correspondence in integrable systems. Two time scales, Ehrenfest time and quantum revival time, are plotted as functions $1/\hbar_\epsilon$. These two time scales mark up three regions: quantum, classical ensemble, and classical. The lines are plotted for the model in eq. (3) with ($x_0 = 0, p_0 = 2$) as the initial condition.

In the end we consider an integrable system of Bose gas for which its effective Planck constant is $1/N$ [20], where N is the total number of the particle. When N is small, the Bose gas is quantum and when N is large it is well approximated by the mean-filed theory [21]. We also find two time scales, the Ehrenfest time scales with N as $N^{1/2}$ and the quantum revival time scales linearly with N. As N can be changed in an experiment, Bose gas offers a potential platform where the scalings of Ehrenfest time and quantum revival time with the Planck constant may be verified experimentally.

2 Ehrenfest time

Before we present our general results, it is illuminating to look at concrete systems with numerical simulation.

2.1 numerical results

We consider the following one dimensional system

$$H = \frac{p^2}{2m} + V(x), \tag{3}$$

where m is the mass of the particle and $V(x) = m\omega_0^2 x^2 + m^2\omega_0^3 x^4/\hbar$. To numerically investigate how Ehrenfest time scales with the Planck constant, we set the Planck constant in the Schrödinger equation as $\tilde{\hbar} = \hbar_\epsilon \hbar$, where the dimensionless constant $\hbar_\epsilon$ is varied. In our numerical calculation, we use $\sqrt{\hbar/(m\omega_0)}$ as unit of length, $\sqrt{\hbar m\omega_0}$ as unit of momentum, $\hbar\omega_0$ as unit of energy, and $1/\omega_0$ as unit of time. In this unit system, $V(x) = x^2 + x^4$.

We compare numerically the quantum and classical dynamics of this system. For a given classical initial condition x_0, p_0, we construct the following Gaussian wave packet as the initial state for the quantum dynamics,

$$\psi(x) = \frac{1}{(2\pi\sigma_x^2)^{1/4}} \exp\left\{-\frac{(x-x_0)^2}{4\sigma_x^2} + \frac{\mathrm{i}p_0(x-x_0)}{\hbar_\epsilon}\right\}, \tag{4}$$

where $\sigma_x = \sqrt{\hbar_\epsilon/2}$. The quantum expectation value $\langle x(t)\rangle$ and the classical trajectory $x_c(t)$ are compared in Figure 2(a). As expected, they match each other for an initial short period of time and then start to deviate. We find that the difference $|\langle x(t)\rangle - x_c(t)|$ oscillates and its peaks can be approximated by function $y = a(1 - \mathrm{e}^{-bt^2})$, as shown in the inset of Figure 2(b). The Ehrenfest time is extracted from these numerical results as $\tau_\hbar = \sqrt{1/b}$. When $\hbar_\epsilon$ is varied, $\tau_\hbar$ varies. Their relation is shown in Figure 2(b), which clearly shows $\tau_\hbar \propto \hbar^{-1/2}$.

In addition, we follow ref. [22] and compare the quantum dynamics to its corresponding classical ensemble evolution. We use the Wigner function of the Gaussian wave packet in

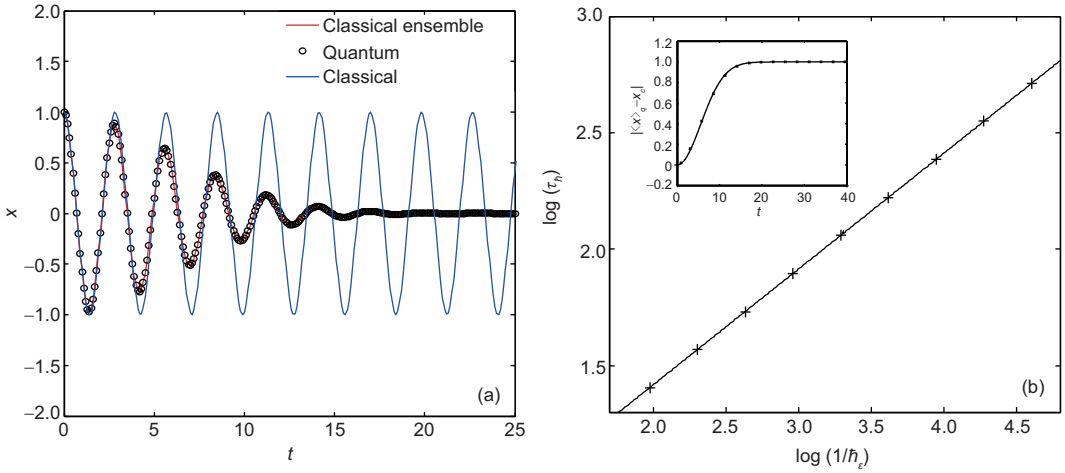

Figure 2 (Color online) (a) The time evolutions of a classical particle $x_c(t)$, its corresponding quantum expectation value $\langle x(t)\rangle$, and the corresponding classical ensemble average $\bar{x}_c(t)$. $x_0 = 1$, $p_0 = 0$, and $\hbar_\epsilon = 0.03$. (b) Relationship between $\tau_\hbar$ and $1/\hbar_\epsilon$, which can be fit by function $y = 0.5x + 0.42$. The inset is a typical fit curve of the evolution of the peaks of the difference between classical value and quantum expectation value. The unit of length is $\sqrt{\hbar/(m\omega_0)}$ and the unit of time is $1/\omega_0$.

eq. (4) as the initial distribution for a classical ensemble

$$\rho_c(x,p) = \frac{1}{\pi\hbar_\epsilon}\exp\left\{-\frac{(x-x_0)^2}{2\sigma_x^2} - \frac{(p-p_0)^2}{2\sigma_p^2}\right\}, \tag{5}$$

where $\sigma_x = \sigma_p = \sqrt{\hbar_\epsilon/2}$. We use $\bar{x}_c$ as the classical ensemble average of x. The agreement between the quantum expectation value $\langle x(t)\rangle$ and $\bar{x}_c(t)$ is almost perfect for a short period of time as shown in Figure 2(a). Such an excellent agreement goes beyond just the averaged value and exists even in phase space. To plot the quantum dynamics in phase space, we use the method in refs. [23, 24] to project wave function unitarily onto quantum phase space. Roughly, the classical phase space is divided into Planck cells and each Planck cell is assigned a Wannier function; these Wannier functions form a complete orthonormal basis which is used for the unitary projection. The results are plotted in Figure 3, where we see that the agreement is excellent within Ehrenfest time and it begins to break only after $t = 26$.

To illustrate that our results hold for higher dimensions, we consider an integrable model of two degrees of freedom. It is a model constructed from three-site Toda lattice [25] with the following Hamiltonian

$$H = \frac{p_1^2}{m} + \frac{p_2^2}{m} + \frac{p_1 p_2}{m} + \mu\left[e^{-x_1/a} + e^{-(x_2-x_1)/a} + e^{x_2/a}\right]. \tag{6}$$

Similarly, we set the Planck constant in the Schrödinger equation as $\tilde{\hbar} = \hbar_\epsilon\hbar$, where the dimensionless constant $\hbar_\epsilon$ can be varied. In our numerical calculation, we use a as unit of length, $\sqrt{m\mu}$ as unit of momentum, μ as unit of energy, and $\hbar/\mu$ as unit of time. In this unit system, $H = p_1^2 + p_2^2 + p_1p_2 + e^{-x_1} + e^{-(x_2-x_1)} + e^{x_2}$. Two independent conserved quantities are H and $F = -(p_1^2p_2 + p_2^2p_1) - p_2e^{-x_1} + (p_1+p_2)e^{-(x_2-x_1)} - p_1e^{x_2}$.

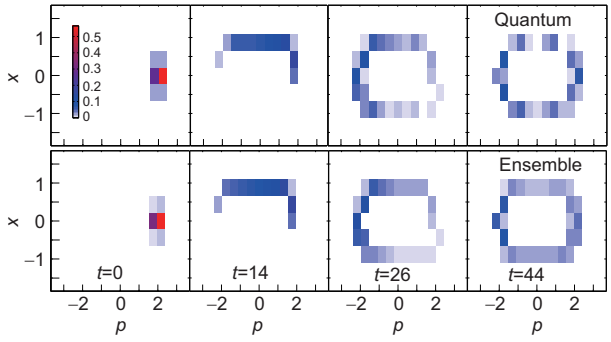

Figure 3 (Color online) Quantum dynamics (upper row) and classical ensemble dynamics (lower row) in phase space. The classical ensemble distribution is coarse-grained to Planck cells. For this case, $\tau_\hbar \approx 26$. ($x_0 = 0$, $p_0 = 2$) and $\hbar_\epsilon = 0.03$. The unit of length is $\sqrt{\hbar/(m\omega_0)}$, the unit of time $1/\omega_0$, and the unit of momentum $\sqrt{\hbar m\omega_0}$.

The computation procedure is similar to the one dimensional case. To determine Ehrenfest time numerically, we use relative difference $|x_{2c}(t) - \langle x_2(t)\rangle|/x_{2c}(t)$ as a criterion. To avoid zero points of $x_{2c}(t)$, we choose time points when $x_{2c}(t)$ is large. As showed in Figure 4, the Ehrenfest time in the two dimensional system also scales with $\hbar$ as $\tau_\hbar \propto \hbar^{-1/2}$.

2.2 General analysis

The numerical results above also indicate that a single-particle classical trajectory deviates from its corresponding classical ensemble dynamics (see Figure 2(a), Figure 4(a) and (b)), which was already noticed in ref. [22]. This fact, together with the perfect agreement between quantum dynamics and classical ensemble dynamics within Ehrenfest time, implies that Ehrenfest time $\tau_\hbar$ is solely caused by the width of a quantum wave packet that has a lower limit set by the

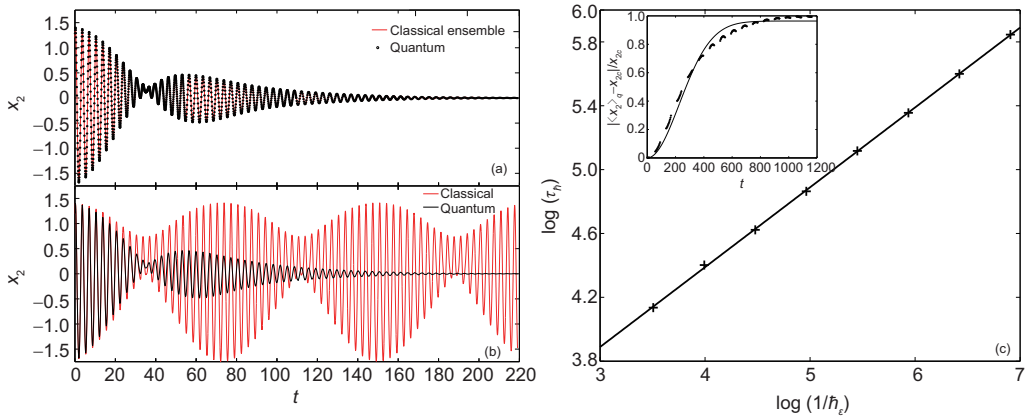

Figure 4 (Color online) Numerical results for the integrable model of two degrees of freedom. (a), (b) The time evolutions of a classical particle position $x_{2c}(t)$, its corresponding quantum expectation value $\langle x_2(t)\rangle$, and the corresponding classical ensemble average $\bar{x}_{2c}(t)$. The initial condition is $x_1 = 0.7, x_2 = 1.2, p_1 = 0.4, p_2 = 0.6$. $\hbar_\epsilon = 0.03$. (c) Relationship between $\tau_\hbar$ and $1/\hbar_\epsilon$, which can be fit by function $y = 0.50x + 2.39$. The inset is a typical fit curve for the evolution of relative difference between classical value and quantum expectation value $|x_{2c}(t) - \langle x_2(t)\rangle|/x_{2c}(t)$. The unit of length is a and the unit of time is $\hbar/\mu$.

uncertainty relation. We exploit it to derive an analytical expression for Ehrenfest time.

We consider a classical ensemble distribution that satisfies the uncertainty relation, such as the one in eq. (5). The evolution of this classical ensemble is governed by Liouville equation, which is totally classical and irrelevant of $\hbar$. The only factor related to $\hbar$ is the fluctuations of position and momentum in this ensemble distribution which are limited by the uncertainty principle.

We choose three points A, B, and C in the phase space such that they initially differ from each other by δp in momentum and δx in position (see Figure 5). In particular, B is the averaged point of A and C. As long as the system is not a harmonic oscillator, these three points have different angular velocities. As time goes by, the average of A and C will differ significantly from B and the correspondence between classical ensemble and classical single particle will break down. When we choose $\delta x \cdot \delta p \sim \hbar$, such a breakdown time is just Ehrenfest time $\tau_\hbar$.

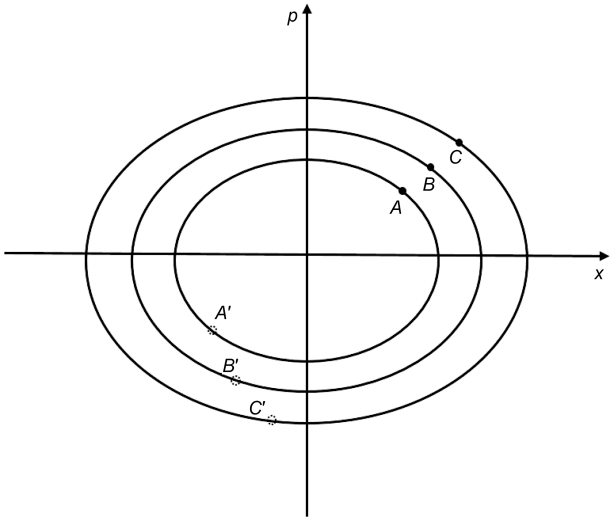

Figure 5 A typical phase space for one dimensional integrable system. Closed curves are energy contours. In general, the oscillation frequencies on different curves are different. So, the three points A, B, and C , initially close to each other, will disperse over time due to different frequencies.

We define $\tau_\hbar$ as the time when the angular difference of A and C is 2π. We thus have

$$\tau_\hbar = \frac{2\pi}{|\omega_A - \omega_C|}, \tag{7}$$

$$\approx \frac{2\pi}{|\omega'(I)| \cdot (|\partial I/\partial x| \cdot \delta x + |\partial I/\partial p| \cdot \delta p)}, \tag{8}$$

where ω is the angular velocity and I is the action. Note that all these quantities $\partial I/\partial p$, $\partial I/\partial x$ and $\omega'(I)$ are classical and independent of $\hbar$. The Planck constant comes in only through the uncertainty relation that requires that $\delta x \sim \delta p \propto \hbar^{1/2}$. So, we have

$$\tau_\hbar \propto \hbar^{-1/2}. \tag{9}$$

There is no need to worry about the possibility $\omega'(I) = 0$ in eq. (8) as it is the result of truncation of the Taylor expansion of $|\omega_A - \omega_C|$ to the first order. If $\omega'(I) = 0$, one just needs to expand it further to the second order. In this case, we would have $\tau_\hbar \propto \hbar^{-1}$. One could continue this expansion until some order becomes non-zero. If all orders of derivative of $\omega(I)$ vanish, the system must be a harmonic oscillator for which $\tau_\hbar$ is indeed infinite.

For n-dimensional integrable system, there exist n pairs of independent action-angle variables and thus n angular velocities, each of which gives a Ehrenfest time according to eq. (8),

$$\tau_{\hbar i} = \frac{2\pi}{|\partial\omega_i/\partial I_j| \cdot (|\partial I_j/\partial x_k| \cdot \delta x_k + |\partial I_j/\partial p_k| \cdot \delta p_k)}, \tag{10}$$

where $i, j, k = 1, 2, ..., n$, and repeated indices imply summation. In phase space, the spread of a wave packet in any direction will cause the break down of the quantum-classical correspondence, so the shortest of them will be Ehrenfest time for the n-dimensional integrable system, that is

$$\tau_\hbar = \min\{\tau_{\hbar i}\}, \qquad (i = 1, 2, \cdots, n). \tag{11}$$

For chaotic systems, it is well accepted that Ehrenfest time $\tau_\hbar = \frac{c}{\gamma} \ln \frac{A}{\hbar}$ [3-9], where γ is the Lyapunov index of the chaotic system, A is a typical action, and c is a dimensionless constant of order one.

However, there is some confusion over Ehrenfest time in integrable systems. Although it is generally believed that for integrable systems Ehrenfest time scales with the Planck constant as $\tau_\hbar \propto \hbar^{-\alpha}$ [26], it is not clear in literature what α is. It was indicated in ref. [11] that $\alpha = 1$ but no detailed explanation was given. It is shown in some specific cases that $\alpha = 1/2$ [26, 27]. Berry [7] studied a similar time scale with Wigner function and found that $\alpha = 2/3$. Combescure and Robert [5] had a general result for integrable systems. They proved that when $t < C\hbar^{-1/2}$, where C is a constant, the quantum evolution of an initially coherent state remains coherent while its center evolves in time according to the classical dynamics. Their result sets a lower bound for Ehrenfest time but does not say how Ehrenfest time should scale with $\hbar$. In fact, any $\alpha \geq 1/2$ would satisfy their lower bound.

Our work clarifies the issue and shows analytically $\alpha = 1/2$ for general integrable systems. In addition, it is clear from our derivation that Ehrenfest time is intrinsic to the system in the sense that it can be understood without referring to a localized initial wave packet as it is the time scale that a classical ensemble distribution in phase space develops structures finer than the Planck cell.

2.3 Examples

We now apply the above result to a couple of examples to get a sense how big or small the Ehrenfest time can become in typical macroscopic and microscopic situations. The first example is a particle of mass m in a one dimensional box of length a. Through some simple calculations we have

$$\tau_\hbar = T_c \sqrt{\frac{2I}{\hbar}}, \tag{12}$$

where $I = pa/\pi$ is the action and $T_c = 2am/p$ is the classical period with p being the momentum of the particle. Here we consider two typical scenarios, one macroscopic and one microscopic. Imagine that a macroscopic ball moves in a box with $m = 1$ g, $a = 1$ m, $v = 1$ m/s. The Ehrenfest time for this system is then $\tau_\hbar = 2.4 \times 10^{15} T_c$. Naturally, classical mechanics is enough to describe such a system. For the microscopic scenario, we consider a ultracold ^{87}Rb atom moving in a optical well [28], where $m = 1.5 \times 10^{-25}$ kg, $v = 10^{-3}$ m/s (estimated under condition $T = 10^{-8}$ K), and $a = 10^{-7}$ m (roughly the wavelength of light). The Ehrenfest time for this case is $\tau_\hbar = 0.8 T_c$. So ultracold atoms must be described by quantum mechanics. This example shows that Ehrenfest time is a good indicator whether a system should be regarded as quantum or classical.

The second example is a system with the inverse square law of force, whose Hamiltonian is

$$H = \frac{p_r^2}{2m} + \frac{L^2}{2mr^2} - \frac{k}{r}, \tag{13}$$

where m is the mass of the object, r is the distance to the center, p_r is the radial momentum, and L is the angular momentum. With canonical transformation, we have

$$H = -\frac{mk^2}{2} \frac{1}{(I + L)^2}, \tag{14}$$

where I is the action variable of the system other than L. To simplify the calculations, we choose a special initial condition $r = \frac{L^2}{mk}$, and the variances of the wave packet are $\delta r = \sqrt{\hbar/(2m\omega)}$, $\delta p_r = \sqrt{m\omega\hbar/2}$, $\delta\theta = \frac{1}{r}\sqrt{\hbar/(2m\omega)}$, and $\delta L = r\sqrt{m\omega\hbar/2}$.

With some simple calculations we have

$$\tau_\hbar = \frac{\sqrt{2}}{3} \frac{T_c}{\sqrt{\frac{\hbar[(I+L)^2 - L^2]}{L^2(I+L)}} + \frac{L}{I+L}\sqrt{\frac{\hbar}{L}}}. \tag{15}$$

For the Sun-Earth system, as the motion is approximately circular motion, we have $I \approx 0$ and $L = 2.7 \times 10^{39} J \cdot s$. So, we have $\tau_\hbar = 2.3 \times 10^{36}$ years while the age of the solar system is just 5×10^9 years. For a hydrogen atom in its ground state, as $L = \hbar$, we have $\tau_\hbar = 0.5 T_c$. This is clearly consistent with our daily experience that we do not need to worry about the quantum effects in the orbits of the solar planets while we have to describe hydrogen atom with quantum mechanics.

3 Quantum revival time

Ehrenfest time gives us the time scale when the quantum dynamics of a single particle deviates from its classical trajectory. However, as shown in Figure 2 and 4, if one compares the dynamics of a quantum wave packet to an ensemble of classical orbits, the quantum-classical correspondence can last much longer. This phenomenon of course has been noticed a long time ago [22]. In this section, we investigate how long the quantum-classical correspondence can last in

this sense. We find that for integrable systems such a time scale is set by quantum revival [17-19] and scales with the Planck constant as $\hbar^{-1}$.

3.1 Numerical results

We further study numerically the quantum dynamic and its corresponding classical ensemble dynamics for much longer times. They are compared in term of the averaged position (see Figure 6) and also in phase space (see Figure 7). If one is only interested in the dynamics of the wave packet center, the quantum and classical ensemble results match each other very well for a very long time, up to $t > 300$ according to Figure 6. After that, around $t \approx 430$, while the classical average $\bar{x}_c(t)$ remains around zero, the quantum expectation $\langle x(t)\rangle$ almost fully recovers its original value, which is known as quantum revival. This quantum revival occurs again when the evolution time is doubled.

However, if one is interested in more dynamical details, the time scale of agreement is shortened by a few fractions. According to Figure 7, after $t = \tau_\hbar \approx 26$, both are no longer localized. However, the quantum distribution always has more structures while the classical ensemble distribution is rather uniformly distributed within the energy shell. In particular, at certain times, one observes that the quantum distribution will cluster around a few centers, a phenomenon known as fractional quantum revival [17]. At $t = 432$, which is half of the quantum revival time, we see that the quantum distribution becomes localized again.

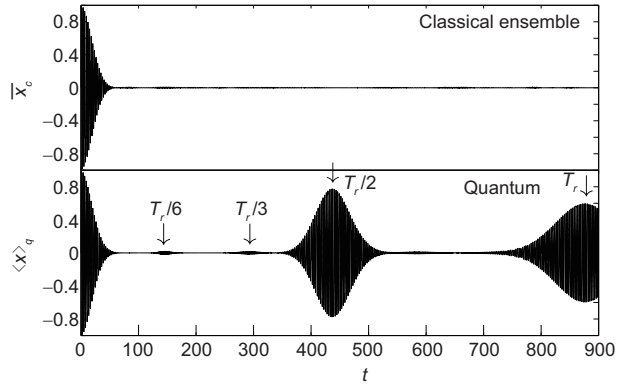

Figure 6 Time evolution of the classical ensemble average $\bar{x}_c(t)$ (upper); time evolution of the quantum expectation value $\langle x(t)\rangle$ (lower). T_r is the quantum revival time. ($x_0 = 0, p_0 = 2$) and $\hbar_\epsilon = 0.03$. The unit of length is $\sqrt{\hbar/(m\omega_0)}$ and the unit of time is $1/\omega_0$.

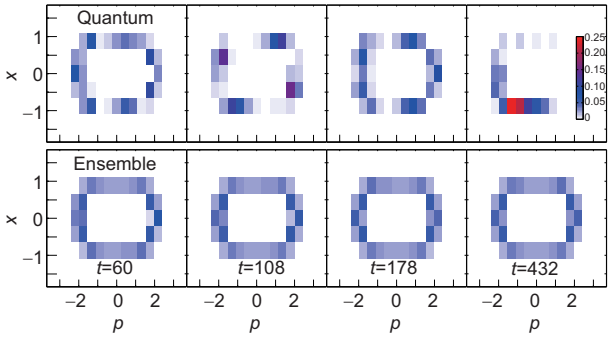

Figure 7 (Color online) Quantum dynamics (upper row) and classical ensemble dynamics (lower row) in phase space. The classical ensemble distribution is coarse-grained to Planck cells. For this case, $T_r \approx 864$ ($x_0 = 0, p_0 = 2$) and $\hbar_\epsilon = 0.03$. The unit of length is $\sqrt{\hbar/(m\omega_0)}$, the unit of time is $1/\omega_0$, and the unit of momentum is $\sqrt{\hbar m\omega_0}$.

3.2 Analytical results

The numerical results above show that quantum dynamics and its corresponding classical ensemble dynamics begin to deviate from each other significantly when quantum revival occurs. In this subsection, we derive an analytic formula for quantum revival time. We follow the method in ref. [17] but with a significant modification by introducing action variables. For a general one dimensional integral system, its classical Hamiltonian can always be written as $H(I)$, where I is the action of the system. As a result, its classical energy is also a function of the action $E(I)$ and so is the classical frequency $\omega(I) = \partial E(I)/\partial I$ [29]. We expand the quantum wave packet in terms of the system's energy eigenstates and its dynamics is then given by

$$\psi(t) = \sum_n c_n e^{-iE_n t/\hbar}\phi_n(x)\,, \tag{16}$$

where $\phi_n(x)$ is the nth eigenstate and E_n is its corresponding energy eigenvalue. The coefficients c_n's are determined by the initial condition. We assume that $|c_m|^2$ is the largest and expand the eigenvalue around E_m as follows:

$$E_n = E_m + \omega(I_m)(I_n - I_m) + \frac{\omega'(I_m)}{2}(I_n - I_m)^2 + ..., \tag{17}$$

where I_n is the action corresponding to E_n via $E(I)$. According to the Bohr-Sommerfeld quantization rule [30], we have

$$I_n - I_m = (n - m)\hbar\,. \tag{18}$$

So, the quantum phases can be written as:

$$\exp\left[-i(E_n - E_m)t/\hbar\right] = \exp\left[-2\pi i(n-m)\frac{t}{T_c} - 2\pi i(n-m)^2\frac{t}{T_r} + ...\right], \tag{19}$$

where $T_c = 2\pi/\omega(I_m)$ and

$$T_r = \frac{4\pi}{\omega'(I_m)\hbar}\,. \tag{20}$$

As T_r contains $\hbar$ in its denominator, it is clear that $T_r \gg T_c$. With this in mind, we can envision from eq. (19) how the

quantum wave packet will evolve in time. For an initial short interval of time, the wave packet will oscillate with period T_c but with a decaying amplitude due to the second-order and other higher order terms. When the evolution time approaches T_r, the second-order terms become multiples of 2π and, as a result, the wave packet recovers most of its original shape. How much it can recover depends on the third and higher order terms and other factors. Before T_r, there can be fractional quantum revivals that occur at $t = pT_r/q$ (p, q are positive integers); they are characterized by a superposition of several localized wave packets [17]. This is exactly what we have observed in Figure 7.

From the above discussion, we find that the quantum revival time T_r scales with the Planck constant as $T_r \propto \frac{1}{\hbar}$. For the two examples mentioned in sect. 2.3, according to eq. (20), we have

$$T_{r1} = T_c \frac{2I}{\hbar}, \tag{21}$$

and

$$T_{r2} = \frac{2}{3} T_c \frac{I+L}{\hbar}, \tag{22}$$

respectively.

We note that the Bohr-Sommerfeld quantization rule is only an approximation; eq. (18) should be corrected to $I_n - I_m = (n-m)\hbar + \delta_e$. For the above analysis to be correct, the condition $\omega(I_m)\delta_e \ll \frac{\omega'(I_m)}{2}(n-m)^2\hbar^2$ should be satisfied. δ_e also affects how much the quantum wave packet can recover its original shape at T_r.

4 Bose gases

It is well known that the relationship between quantum and mean field descriptions of Bose gases is essentially quantum-classical correspondence [19-21] with $1/N$ (N is the total number of bosons) serving as effective Planck constant. Our results above can be straightforwardly applied to any system of Bose gas which is integrable as it was done for the chaotic Bose system in ref. [21]. We illustrate this with a two-site Bose-Hubbard model as an example, whose Hamiltonian is

$$\hat{H} = -\frac{\nu}{2}(\hat{a}^\dagger \hat{b} + \hat{a}\hat{b}^\dagger) + \frac{c}{2N}(\hat{a}^\dagger \hat{a}^\dagger \hat{a}\hat{a} + \hat{b}^\dagger \hat{b}^\dagger \hat{b}\hat{b}), \tag{23}$$

where with $\hat{a}^\dagger(\hat{a})$ and $\hat{b}^\dagger(\hat{b})$ the creation (annihilation) operators in well a and b, c is the strength of interaction and ν is the tunneling parameter. In our numerical calculation, we use ν as unit of energy, $\hbar/\nu$ as unit of time. When the particle number N is large, this system can be well approximated by the following mean field model

$$H_{\rm mf} = -\frac{\nu}{2}(a^* b + a b^*) + \frac{c}{2}(|a|^4 + |b|^4). \tag{24}$$

Owing to the particle number conservation, $|a|^2 + |b|^2 = 1$, and the overall phase is trivial, we can introduce a pair of conjugate variables s and θ, where $s = |b|^2$, $\theta = \theta_b - \theta_a$ with θ_b and θ_a being the phases of complex numbers a and b. The mean field model is clearly a classical one dimensional integrable system.

In the above discussion of quantum-classical correspondence of a single particle, a point in the classical phase space corresponds to a Gaussian wave packet of minimal spread. For this Bose system, a mean field state $a = \alpha$, $b = \beta$ corresponds to a quantum coherent state $|\alpha, \beta\rangle$

$$|\alpha, \beta\rangle = \frac{1}{\sqrt{N!}}(\alpha a^\dagger + \beta b^\dagger)^N |0\rangle, \tag{25}$$

where $|0\rangle$ is the vacuum state.

However, we need some effort to construct the corresponding mean field ensemble distribution $\rho(s, \theta)$. We expand the coherent state $|\alpha, \beta\rangle$ with Fock states $|n, N-n\rangle$, where n is the particle number at site a,

$$|\alpha, \beta\rangle = \sum_s \varphi_N(s) |N - Ns, Ns\rangle, \tag{26}$$

where

$$\varphi_N(s) = \sqrt{\frac{N!}{Ns!(N-Ns)!}} \alpha^{N-Ns} \beta^{Ns}, \tag{27}$$

and s ranges over $0/N, 1/N, ..., N/N$. $|\varphi_N(s)|^2$ can be regarded as a distribution of s. For this distribution, the average of s is $\bar{s} = |\beta|^2$ and its variance is

$$\Delta s = \frac{|\beta| \sqrt{(1-|\beta|^2)}}{\sqrt{N}}. \tag{28}$$

As θ is the conjugate of s, its distribution can be obtained with a Fourier transform

$$\phi_N(\theta) = \frac{1}{\sqrt{N+1}} \sum_s \varphi_N(s) e^{-iNs\theta}, \tag{29}$$

where θ takes the following discrete values: $2\pi\frac{1}{N+1}$, $2\pi\frac{2}{N+1}$, ..., $2\pi\frac{N+1}{N+1}$. Numerical results show that

$$\bar{\theta} \approx \theta_\beta - \theta_\alpha, \qquad \Delta\theta \approx \frac{1}{2\sqrt{N}|\beta|\sqrt{(1-|\beta|^2)}}. \tag{30}$$

So, $\Delta\theta$ and Δs satisfy the uncertainty relation: $\Delta\theta\Delta s \approx \frac{1}{2N}$. At the large N limit, $N \to +\infty$, both $|\varphi_N(s)|^2$ and $|\phi_N(\theta)|^2$ will approach Gaussian distribution. If we denote these two Gaussian distributions as $g_1(s)$ and $g_2(\theta)$, respectively, the mean-field ensemble distribution can be constructed as $\rho(s, \theta) = g_1(s) g_2(\theta)$. The three different dynamics, mean-field, mean-field ensemble, and quantum, are compared in Figure 8. We find a very similar pattern as we found in sect. 2 and sect. 3.

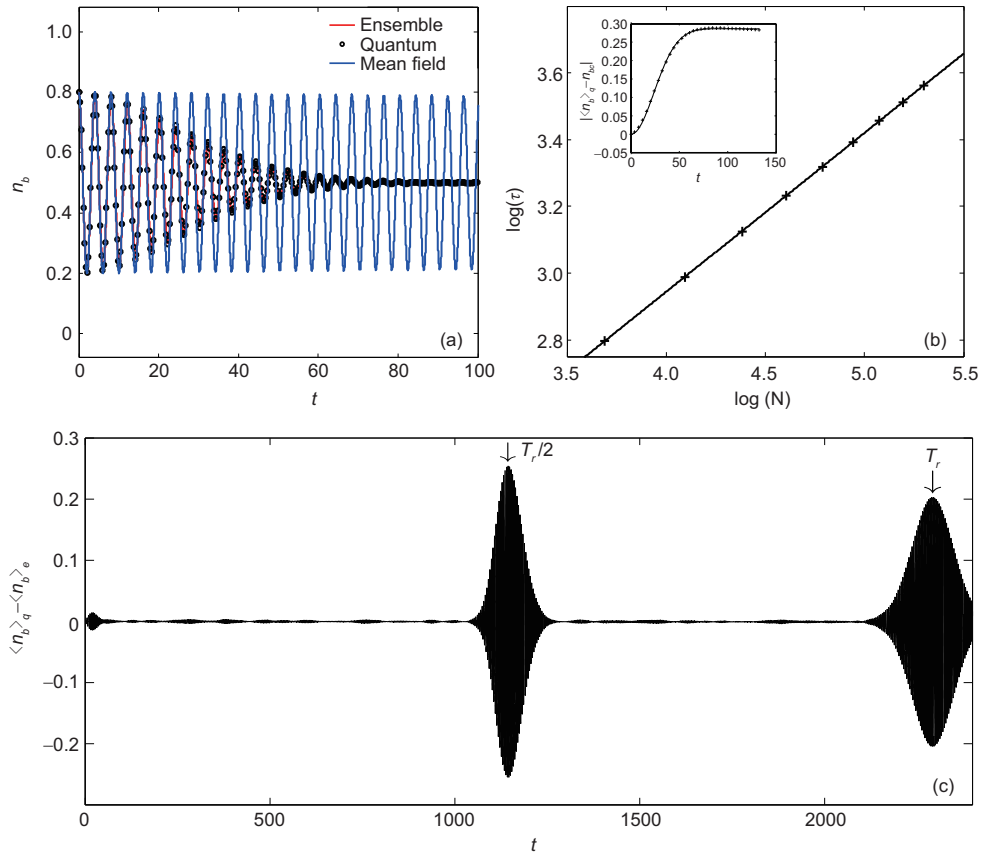

Figure 8 (Color online) (a) The time evolution of the averaged probability of the system in state b according to three different dynamics: quantum, mean-field, and mean field ensemble. (b) Ehrenfest time as a function of number of particles N, which can be fitted by $y = 0.48x + 1$. The inset is a typical fit curve of the evolution of the peaks of the difference between averaged probability in state b according to mean field and quantum dynamics. (c) The evolution of difference between quantum expectation value and mean field ensemble average of occupation probability at state b. $N = 200$, $c/\nu = 2$. The unit of time is $\hbar/\nu$.

For quantum revival, we would need the Bohr-Sommerfeld quantization rule. How to implement this rule in the mean field theory of a Bose gas is discussed in refs. [31,32].

In conclusion, the breakdown of correspondence between quantum and mean field descriptions occurs at time $\tau_\hbar \propto N^{1/2}$, and the breakdown of correspondence between quantum and mean field ensemble occurs at time $T_r \propto N$. The Planck constant $\hbar$ can not be changed experimentally, but the total number of bosons N can. Therefore, the Bose gases can be used to experimentally verify the results in this paper.

5 Discussion and conclusion

In summary, we have shown that for a generic integrable system there exist two different time scales, Ehrenfest time $\tau_\hbar \propto \hbar^{-1/2}$ and quantum revival time $T_r \propto \hbar^{-1}$. When they are plotted in Figure 1, they mark up three different regions in the space spanned by $\hbar$ and dynamical evolution time t. In the classical region, a narrow quantum wave packet does not spread much and its center follows the classical particle trajectory. In the classical ensemble region, a quantum wave packet can be regarded as a classical ensemble distribution in phase space. In the quantum region, quantum revival occurs and the quantum dynamics can not even be approximated with classical ensemble.

We call Figure 1 Ehrenfest diagram for two reasons. The first is to honor Ehrenfest for his pioneering work on quantum-classical correspondence [2]. The second and more important reason is that we expect the prominent feature, three different regions marked up by two different time scales, in Figure 1 to be generic. Even for chaotic systems, this feature is expected to persist; the difference is that the Ehrenfest time becomes logarithmic and the quantum revival time will be replaced by other quantum times that scale with $\hbar$ differently. For example, for quantum kicked rotor, the second time is the time scale for dynamical localization or quantum resonance and it scales as $\hbar^{-2}$ [33]. We may call this second time scale quantum time. We note that this quantum time in our integrable systems is not Heisenberg time: as indicated in eq. (19), the quantum revival comes from the second-order terms in the eigen-energy expansion.

It would be very interesting to see how this kind of Ehrenfest diagram evolves when a system changes from integrable

to chaotic. It is not clear how Ehrenfest time changes from square root to logarithmic. For a chaotic system, the quantum revival time is likely exponentially long, so the quantum time in the chaotic system must have a different cause. It is not clear what the cause is or whether this cause may change from system to system.

We acknowledge helpful discussion with Yuan Fang on plotting Figure 3 and 7. This work was supported by the National Key Research and Development Program of China (Grant Nos. 2017YFA0303302, and 2018YFA0305602), and the National Natural Science Foundation of China (Grant Nos. 11334001, and 11429402).

1 M. C. Gutzwiller, *Chaos in Classical and Quantum Mechanics* (Springer, New York, 1990).
2 P. Ehrenfest, Zeitschrift Physik A Hadrons Nuclei **45**, 455 (1927).
3 G. P. Berman, and G. M. Zaslavsky, Phys. A-Stat. Mech. Appl. **91**, 450 (1978).
4 G. M. Zaslavsky, Phys. Rep. **80**, 157 (1981).
5 M. Combescure, and D. Robert, Asympt. Anal. **14**, 377 (1997).
6 G. A. Hagedorn, and A. Joye, Ann. Henri Poincaré **1**, 837 (2000).
7 M. V. Berry, J. Phys. A-Math. Gen. **12**, 625 (1979).
8 P. G. Silvestrov, and C. W. J. Beenakker, Phys. Rev. E **65**, 035208 (2002).
9 C. Tian, A. Kamenev, and A. Larkin, Phys. Rev. B **72**, 045108 (2005).
10 D. R. Grempel, S. Fishman, and R. E. Prange, Phys. Rev. Lett. **53**, 1212 (1984).
11 S. Fishman, D. R. Grempel, and R. E. Prange, Phys. Rev. A **36**, 289 (1987).
12 Y. C. Lai, E. Ott, and C. Grebogi, Phys. Lett. A **173**, 148 (1993).
13 M. L. Du, and J. B. Delos, Phys. Rev. Lett. **58**, 1731 (1987).
14 M. Du, and J. Delos, Phys. Rev. A **38**, 1896 (1988a).
15 M. Du, and J. Delos, Phys. Rev. A **38**, 1913 (1988b).
16 J. B. Delos, and M. L. Du, IEEE J. Quantum Electron. **24**, 1445 (1988).
17 R. Robinett, Phys. Rep. **392**, 1 (2004).
18 A. Bakman, H. Veksler, and S. Fishman, Phys. Lett. A **381**, 2298 (2017), arXiv: 1606.02923.
19 H. Veksler, and S. Fishman, New J. Phys. **17**, 053030 (2015), arXiv: 1409.5115.
20 L. G. Yaffe, Rev. Mod. Phys. **54**, 407 (1982).
21 X. Han, and B. Wu, Phys. Rev. A **93**, 023621 (2016), arXiv: 1506.04020.
22 L. E. Ballentine, Y. Yang, and J. P. Zibin, Phys. Rev. A **50**, 2854 (1994).
23 X. Han, and B. Wu, Phys. Rev. E **91**, 062106 (2015).
24 Y. Fang, F. Wu, and B. Wu, J. Stat. Mech. **2018(2)**, 023113 (2018), arXiv: 1708.06507.
25 M. Toda, J. Phys. Soc. Jpn. **22**, 431 (1967).
26 G. P. Berman, E. N. Bulgakov, and D. D. Holm, *Crossover-time in Quantum Boson and Spin Systems* (Springer-Verlag, Berlin, 1994), vol. 21.
27 G. P. Berman, A. M. Iomin, and G. M. Zaslavsky, Phys. D-Nonlinear Phenom. **4**, 113 (1981).
28 F. Dalfovo, S. Giorgini, L. P. Pitaevskii, and S. Stringari, Rev. Mod. Phys. **71**, 463 (1999).
29 V. I. Arnold, *Mathematical Methods of Classical Mechanics* (Springer-Verlag, New York, 1978).
30 A. Messiah, *Quantum Mechanics* (Dover, New York, 1999).
31 B. Wu, and J. Liu, Phys. Rev. Lett. **96**, 020405 (2006).
32 X. Luo, Q. Xie, and B. Wu, Phys. Rev. A **77**, 053601 (2008), arXiv: 0712.1257.
33 F. M. Izrailev, Phys. Rep. **196**, 299 (1990).